

# Position-Space Description of the Cosmic Microwave Background and Its Temperature Correlation Function

Sergei Bashinsky<sup>1</sup> and Edmund Bertschinger<sup>2</sup>

<sup>1</sup>Center for Theoretical Physics, <sup>2</sup>Center for Space Research, and <sup>1,2</sup>Department of Physics, Massachusetts Institute of Technology, Cambridge, Massachusetts 02139

December 7, 2000

We suggest that the angular CMB temperature correlation function  $C(\theta)$  provides a direct and practical connection between the experimental data and the fundamental cosmological quantities. Evolution of inhomogeneities in the pre-recombination universe is studied using their Green's functions in position space. We find that a primordial adiabatic point perturbation propagates as a sharp-edged spherical acoustic wave. Density singularities at the wave front give rise to a feature in the CMB correlation function distinguished by a dip at  $\theta \approx 1.2^\circ$ . Characteristics of the feature are sensitive to the cosmological parameter values, in particular to the total and the baryon densities.

The cosmic microwave background (CMB) radiation provides the best probe today of the early universe and a number of fundamental astrophysical constants [1–7]. Dynamical evolution of primordial perturbations manifests itself in the form of “acoustic peaks” in the CMB temperature angular power spectrum  $C_l$ . After over a decade of studies, the physical content of the peaks has become qualitatively understood [8–11]. Nevertheless, one has to rely on standard numerical codes [12,13] to establish a quantitative connection between CMB anisotropy and cosmological parameters. This connection is particularly important now that high-precision CMB measurements have become reality, and that the Boomerang [14] and MAXIMA [15] experiments suggest a baryon density higher than is compatible with big bang nucleosynthesis [16].

How can one deduce the cosmological parameters and the physical processes underlying the observed pattern of CMB anisotropy? When the microwave background photons were last scattered, the magnitude of density fluctuations was only  $O(10^{-5})$ , justifying a perturbative analysis. Fourier expansion of the spatial inhomogeneities has traditionally been the starting point of cosmological perturbation theories [17–19].

In this Letter we show that many previously unnoticed physical phenomena are unraveled by considering the dynamics of interacting matter and gravitational fields in position rather than Fourier space. A position-space formalism may provide practical gains as well. The currently used techniques would require unreasonably long time [20] to calculate the  $C_l$  spectrum for the vast amount of data expected from future large CMB experiments. Szapudi *et al.* [21] have recently developed methods that make the data analysis tractable using the angular temperature correlation function  $C(\theta)$ . Here we demonstrate using the simple dynamics of perturbations in position space that primordial inflationary fluctuations produce a sharp feature in the angular correlation function. This signature may enable an even cleaner extraction of physical quantities from  $C(\theta)$  than from  $C_l$ .

As a simplified model of the dynamics essential to CMB on experimentally accessible scales, we consider a photon-baryon and cold dark matter two-fluid system. The photon gas is assumed to be tightly coupled to electrons and baryons by Thomson scattering until the latter recombine at redshift  $z_{\text{rec}} \sim 1100$ . The disregard of neutrino free-streaming and photon diffusion introduces a 10%–20% error [22,23] for CMB temperature anisotropy. This model is helpful for developing understanding. Our numerical results for the correlation function and the angular spectrum use a full calculation with CMBFAST [12] and include all relevant effects.

Long before recombination during the radiation era, the evolution of adiabatic perturbation modes in Fourier space is described by known analytical formulas, e.g. eq. (5.7) in [17]. A delta-function primordial isentropic perturbation  $\delta^{(3)}(\vec{x})$  corresponds to constant initial gravitational potential amplitude in  $k$ -space,  $\phi(\vec{k}, \tau \rightarrow 0) \equiv 1$ . The Fourier transform of  $\phi(\vec{k}, \tau)$  gives the three-dimensional Green's function for the gravitational potential at  $z \gg z_{\text{eq}} \simeq 2.4 \times 10^4 \Omega_m h^2$ ,

$$\phi^{(3)}(r, \tau) = \frac{3}{4\pi} (c_s \tau)^{-3} \theta(c_s \tau - r), \quad (1)$$

where  $\theta(x) = \{1, x > 0; 0 \text{ otherwise}\}$ ,  $\tau$  is the conformal time,  $c_s = 1/\sqrt{3}$  is the sound speed in the radiation epoch, and we use the conformal Newtonian gauge [19,24] to describe gravity. This result illustrates the essential property of the position-space transfer functions. The perturbation is localized within the acoustic sphere, with a sharp edge at the sound horizon  $s = \int_0^\tau c_s(\tau') d\tau'$ .

When cold dark matter (CDM) and baryons are taken into account, we split the total gravitational potential  $\phi = \phi_r + \phi_c$  into a part connected to the photon-baryon plasma,  $\phi_r$ , and a part due to the CDM,  $\phi_c$ . The sources of the potentials  $\phi_r$  and  $\phi_c$  are given respectively by the radiation-baryon and CDM energy densities relative to the net zero-momentum hypersurfaces, the analogues of Bardeen's [17] gauge-invariant density variable  $\epsilon_m$ . The evolution of the radiation and CDM fluids is described by a pair of coupled equations,

$$\begin{aligned}\ddot{\phi}_r + \sum_{i=r,c} (A_{ri}\dot{\phi}_i + B_{ri}\phi_i) &= c_s^2 \nabla^2 \phi_r, \\ \ddot{\phi}_c + \sum_{i=r,c} (A_{ci}\dot{\phi}_i + B_{ci}\phi_i) &= 0\end{aligned}\quad (2)$$

where  $A_{ij}$  and  $B_{ij}$  are certain rational functions of  $\tau$ . Perturbations in the radiation component propagate with a speed given by  $c_s^2 = dp_\gamma/d(\rho_\gamma + \rho_b) = (1/3)/[1 + (3\rho_b)/(4\rho_\gamma)]$  where  $\rho_\gamma$  and  $\rho_b$  are the photon and baryon mean densities. This speed exceeds the “adiabatic acoustic” speed  $c_a^2 = dp_{\text{tot}}/d\rho_{\text{tot}} = (1/3)/[1 + (3\rho_m)/(4\rho_r)]$ ,  $\rho_m = \rho_{\text{CDM}} + \rho_b$  and  $\rho_r = \rho_\gamma + \rho_\nu$ , because the abundant cold dark matter component does not directly participate in the perturbation propagation. At recombination  $c_s/c_a \simeq 1.5$ .

The values of all the density and velocity perturbations are determined in our model by  $\phi_r$  and  $\phi_c$  through the total gravitational potential  $\phi$  and the entropy potential

$$\sigma = \frac{\rho_m}{\rho_r} \left[ \left( \frac{c_s^2}{c_a^2} - 1 \right) \phi_r - \phi_c \right] \quad (3)$$

defined by  $\nabla^2 \sigma \equiv 3(\delta p - c_a^2 \delta \rho)/(2\rho_m c_a^2 \tau_0^2)$ , where  $\tau_0 \equiv H_0^{-1} (1 + z_{\text{eq}})^{-1/2} \Omega_m^{-1/2}$  characterizes the time of matter and radiation density equality.

From eqs. (2), a primordially isentropic perturbation at a point propagates as a spherical acoustic wave in the photon-baryon plasma with the sound speed  $c_s$ . As the sound wave passes by, the gravitationally coupled CDM becomes perturbed and undergoes local evolution described by the potential  $\phi_c$ . The dynamical motion differs for the two components and the isentropic condition  $\sigma = 0$  does not hold for  $\tau > 0$ .

Eqs. (2) can be efficiently integrated numerically along the characteristics starting from the exact radiation-era solution. An important technical point needs to be made here: The Green’s function initial condition in three dimensions, eq. (1), is inconvenient for numerical integration because it results in highly singular density transfer functions. The singularities are alleviated enabling a simpler numerical treatment if we use one-dimensional, or plane-parallel, Green’s functions for eqs. (2) such that  $\phi^{(1)}(x, \tau \rightarrow 0) = \delta(x)$ . They are related to the three-dimensional, spherical, Green’s functions by a Huygens’ construction

$$\phi^{(1)}(x) = \int_{|x|}^{\infty} 2\pi r dr \phi^{(3)}(r) \quad (4)$$

and they contain the same information. The 1D Fourier transform of  $\phi^{(1)}(x)$  and the 3D transform of  $\phi^{(3)}(x)$  both result in the same conventional  $k$ -space transfer function  $\phi(k)$ . Hereafter, we call the one-dimensional Green’s functions the transfer functions in position space.

The position space approach provides a powerful consistency test for the transfer function calculations. The  $dx$  integrals of any potential, density, or velocity perturbation Green’s function evolves with time according

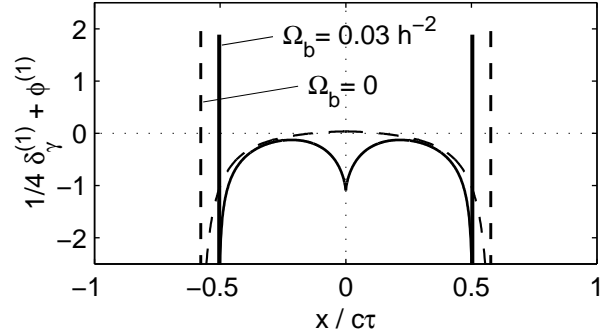


FIG. 1. The position space transfer function for the intrinsic  $(\frac{1}{4}\delta_\gamma)$  plus gravitational redshift contributions to the CMB temperature anisotropy  $\Delta T/T$  with  $\Omega_m = 0.35$ ,  $\Omega_\Lambda = 0.65$ , and  $h = 0.65$ . The vertical spikes represent the wave-front  $\delta$ -function singularities described in the text. Baryon drag effects are evident from comparing the solid and dashed lines.

to homogeneous (space independent) perturbation equations. Such  $k = 0$  perturbations are strictly isentropic for the adiabatic initial conditions and are exactly solvable. These “sum rules” are effective for checking the analytic formulas, debugging the code, and estimating the accuracy of the numerical calculations.

Fig. 1 shows the result for the position-space transfer function describing the combined intrinsic and gravitational redshift contributions to the CMB temperature anisotropy. This transfer function is singular at the wave fronts with the singularities given analytically by  $(3/4)[1 + (3\rho_b)/(4\rho_\gamma)]^{-1/4} \delta(s - |x|)$ ,  $s \equiv \int_0^\tau c_s(\tau') d\tau'$ . For the parameters choice of Fig. 1, the relative contributions of the singular and the regular pieces into their overall integral over  $dx$  are approximately 3.5 and -2.5, implying that the singularities play a major role in the perturbation evolution.

The massive baryons coupled to the radiation fluid decrease the sound speed, shrinking the acoustic horizon at recombination. They also reduce the photon density in regions with positive CDM potential  $\phi_c$ , causing the “gully” in the middle of the transfer function in Fig. 1. The gully arises because non-relativistic baryons are repelled by a positive kink in  $\phi_c^{(1)}$  at  $x = 0$  and they drag the photons out of the central region.

The finite extent of the position-space Green’s functions results in oscillations in their Fourier transforms, the momentum space transfer functions. These oscillations appear as the famous acoustic peaks in the CMB angular spectrum  $C_l$ . The characteristic period of the acoustic oscillations is  $\Delta l = \pi r/s \simeq 300$  for  $\Omega_m = 0.35$ ,  $\Omega_\Lambda = 0.65$  and the Hubble constant  $h = 0.65$  with  $r \simeq 14$  Gpc, the comoving distance to the photosphere at recombination.

The peculiar features of the position space transfer functions are manifested more clearly in the untransformed angular correlation function

$$C(\theta) \equiv \langle \Delta T(\hat{n}_1) \Delta T(\hat{n}_2) \rangle = \sum_l \frac{(2l+1)}{4\pi} C_l P_l(\cos \theta) , \quad (5)$$

where  $\Delta T(\hat{n}_i)$  is the temperature anisotropy in the direction  $\hat{n}_i$ , and  $\theta$  is the angle between  $\hat{n}_1$  and  $\hat{n}_2$ . First of all, the  $\delta$ -function singularities produce a characteristic  $(q-1) \ln |q-1| + \text{const}$ ,  $q(\theta) = \sin(\theta_s/2)/\sin(\theta/2)$  and  $\sin(\theta_s/2) \equiv s/r$ , behavior in the vicinity of  $\theta_s$ . When

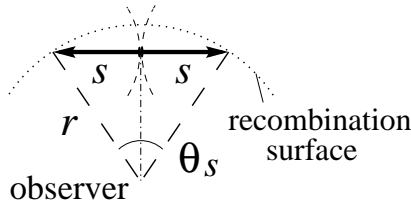


FIG. 2. The feature in  $C(\theta)$  occurs when the observed points establish acoustic contact. Their temperature correlation is then suddenly affected by all the short-wavelength tail of the primordial fluctuation spectrum. The observed critical angle  $\theta_s$  depends on the acoustic horizon size, distance to the CMB photosphere, and the cosmic curvature.

the two observed points come into acoustic contact at the critical angle  $\theta_s$ , as in Fig. 2, we have the case that  $dC(\theta_s)/d\theta = +\infty$ , in the approximation of instantaneous recombination.

Paradoxically, initial acoustic contact anti-correlates the temperature fluctuations causing a *dip* in the correlation function just below  $\theta_s$ . As evident from Fig. 3, the dip is present in the result obtained from a full CMBFAST calculation as well (wide solid line) although smoothed by the Silk damping [25] and the finite thickness of the recombination photosphere. An anomaly in the correlation function at this angular separation was pointed out earlier in [26] and [27]. At even smaller angles the correlation function rises steeply. The dip occurs when the comoving coordinate separation is about  $2s(\tau_{\text{rec}})$  (see Fig. 2), providing a “standard ruler” in the early universe. The corresponding observed angle is determined by the rate of the subsequent Hubble expansion and the cosmic curvature. In particular, it depends on the total density parameter  $\Omega$ . The dash-dotted line in Fig. 3 demonstrates the shift in the visible location of the feature for an open model.

What is the origin of the dip in the correlation function at the acoustic contact? From eq. (4), the intrinsic temperature Green’s function in three dimensions is given by the  $x$  derivative of the corresponding function from Fig. 1 and contains derivatives of delta functions. The latter probe the gradient of the primordial potential rather than its magnitude and contribute with opposite signs to the temperatures at the observed points.

For  $\theta \lesssim \theta_s/2$  the correlation function slope becomes sensitive to the baryon density  $\Omega_b$ . This can be seen from comparing the dashed and solid lines in Fig. 3. At such a small angular separation, the Doppler and the integrated

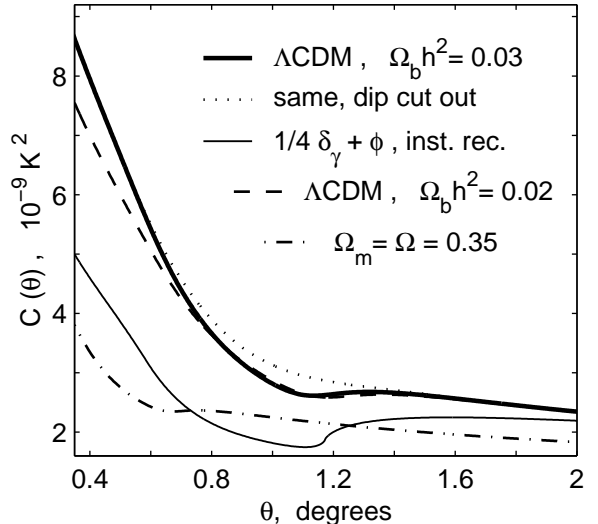


FIG. 3. Angular CMB temperature correlation function. The parameters for the  $\Lambda$ CDM model are  $\Omega_m = 0.35$ ,  $\Omega_\Lambda = 0.65$ ,  $h = 0.65$ ,  $n_{\text{scalar}} = 1$ . For this set of parameters and the displayed  $\Omega_b h^2$  values,  $\theta_s \simeq 1.17^\circ$  and  $1.22^\circ$ . The thin solid curve is calculated using only the temperature transfer function from Fig. 1 and assuming instantaneous recombination. All the other plots are obtained in full CMBFAST calculation, except for the dotted line that artificially cuts the dip for its Fourier analysis in Fig. 4. The whole feature in  $C(\theta)$  is shifted to smaller angles in the open model (dash-dotted line). Baryon density variation modifies the slope for  $\theta < \theta_s/2$  (dashed vs. solid line).

Sachs-Wolfe effects provide significant contribution to the temperature correlation. Nevertheless, the  $\Omega_b$  dependence is largely determined by the same intrinsic plus gravitational redshift contributions shown in Fig. 1. The correlation  $C(\theta) = \langle \Delta T(\hat{n}_1) \Delta T(\hat{n}_2) \rangle$  is a certain convolution of the primordial fluctuation spectrum and two transfer functions for  $\Delta T(\hat{n}_1)$  and  $\Delta T(\hat{n}_2)$ . It is the interference of the  $\delta$ -function singularities and the baryon-induced “gully” in the middle of the transfer functions that causes the break in  $C(\theta)$  at  $\theta \approx \theta_s/2$ . The effect is almost linearly proportional to  $\Omega_b h^2$  and is useful for measuring the baryon density value using CMB data.

How are the position-space features related to the angular power spectrum  $C_l$ ? The solid line in Fig. 4 is the familiar angular spectrum corresponding to the first  $\Lambda$ CDM model from Fig. 3. The dotted line gives  $C_l$  when the dip in  $C(\theta)$  is artificially cut out and replaced by a smooth interpolation with no local minimum, as shown by dots in Fig. 3. This operation eliminates all the acoustic peaks besides the first one. The first peak is closely connected with the sharp rise in  $C(\theta)$  at smaller angles. Increasing the baryon density we increase the slope of  $C(\theta)$ . The magnitude of the first peak grows accordingly (dashed vs. solid lines in Fig. 4) leading to the known [10] reduction in the ratio of second to first acoustic peaks.

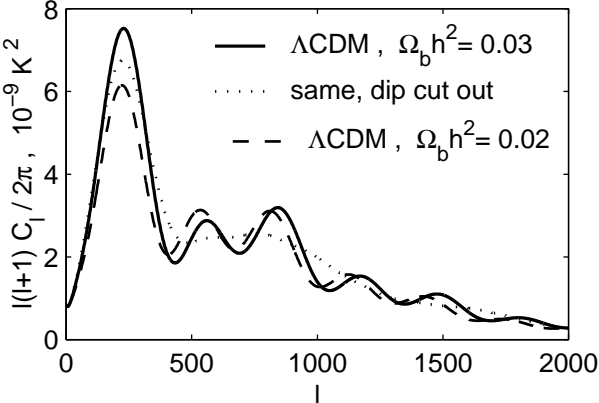


FIG. 4. Angular power spectra for the  $\Lambda$ CDM models of Fig. 3. The dotted line gives  $C_l$  corresponding to the correlation function of the first model with the dip cut out.

We conclude that the Green's function method provides a promising alternative to the conventional Fourier analysis of perturbations in the early universe. It offers new analytical methods and gives new intuition for the familiar phenomena such as the acoustic oscillations or the dependence of peak ratios on  $\Omega_b h^2$ . It also reveals new features that are localized and easily noticeable in position space but which were stretched over a multitude of wavenumbers in the Fourier domain. Examples are the transfer function singularities that result in potentially measurable features in the CMB correlation function.

In this Letter we have discussed only adiabatic (curvature) perturbations. A Green's function approach is even more natural for isocurvature and defect models [28], where it was considered earlier [29].

Our method may have computational advantages compared with Fourier space approaches in that integration effort is concentrated within compact regions of space. We numerically integrate eqs. (2) from  $\tau_{\text{init}} \simeq 10^{-4} \tau_{\text{rec}}$  and increase space-time grid spacing in proportion to the acoustic horizon size  $s$ . Computation of the transfer function in Fig. 1 takes less than one second for 0.01% numerical accuracy on a PC. We are working to extend the method to integration of the Boltzmann equation for free-streaming neutrinos and photons after recombination.

We believe that one of the most promising applications resides in the CMB data analysis [21], where the expense of the traditional Fourier method limits the maximum multipole reached by the Boomerang data [14] and will do so even more so for upcoming satellite experiments [20]. The features in the angular correlation function can be parameterized and estimated quickly and directly from CMB maps. Conversion of real-space measured data into the Fourier domain would become unnecessary. A good parameterization could lead to a small number of nearly sufficient statistics, enabling further speedup in the data analysis.

We thank J. Bond, K. Burgess, D. Pogosyan, and

A. Shirokov for helpful comments and discussion, and gratefully acknowledge the hospitality of CITA where part of this work was performed. Support was provided by NSF grant AST-983137 and by the U. S. Department of Energy under cooperative research agreement DF-FC02-94ER40818.

- 
- [1] L. Knox and L. Page, Phys. Rev. Lett. **85**, 1366 (2000).  
[2] A. H. Jaffe *et al.*, astro-ph/0007333.  
[3] M. Tegmark and M. Zaldarriaga, Phys. Rev. Lett. **85**, 2240 (2000); M. Tegmark, M. Zaldarriaga and A. J. Hamilton, astro-ph/0008167.  
[4] W. Hu *et al.*, astro-ph/0006436.  
[5] S. Dodelson and L. Knox, Phys. Rev. Lett. **84**, 3523 (2000).  
[6] N. Bahcall *et al.*, Science **284**, 1481 (1999).  
[7] J. R. Bond, G. Efstathiou and M. Tegmark, MNRAS **291**, L33 (1997).  
[8] W. Hu, N. Sugiyama, and J. Silk, Nature **386**, 37 (1997).  
[9] W. Hu and M. White, Astrophys. J. **471**, 30 (1996).  
[10] W. Hu and N. Sugiyama, Astrophys. J. **444**, 489 (1995).  
[11] M. White, D. Scott, and J. Silk, Ann. Rev. Astron. Astrophys. **32**, 319 (1994).  
[12] U. Seljak and M. Zaldarriaga, Astrophys. J. **469**, 437 (1996).  
[13] A. Lewis, A. Challinor, and A. Lasenby, Astrophys. J. **538**, 473 (1999).  
[14] P. de Bernardis *et al.*, Nature (London) **404**, 995 (2000).  
[15] S. Hanany *et al.*, astro-ph/0005123.  
[16] S. Burles, K. M. Nollett, and M. S. Turner, astro-ph/0008495; M. Kaplinghat and M. S. Turner, astro-ph/0007454.  
[17] J. M. Bardeen, Phys. Rev. **D22**, 1882 (1980).  
[18] H. Kodama and M. Sasaki, Prog. Theor. Phys. Suppl. **78**, 1 (1984), Int. J. Mod. Phys. **A2**, 491 (1987).  
[19] V. F. Mukhanov, H. A. Feldman, and R. H. Brandenberger, Phys. Rept. **215**, 203 (1992).  
[20] J. R. Bond *et al.*, astro-ph/9903166.  
[21] I. Szapudi *et al.*, astro-ph/0010256.  
[22] U. Seljak, Astrophys. J. Lett. **435**, L87 (1994).  
[23] W. Hu, D. Scott, N. Sugiyama, and M. White, Phys. Rev. **D52**, 5498 (1995).  
[24] C.-P. Ma and E. Bertschinger, Astrophys. J. **455**, 7 (1995).  
[25] J. Silk, Astrophys. J. **151**, 459 (1968).  
[26] A. A. Starobinskii, Sov. Astron. Lett. **14** 3, 166, (1988).  
[27] H. E. Jorgensen *et al.*, Astron. Astrophys. **294**, 639 (1995).  
[28] A. Albrecht *et al.*, Phys. Rev. Lett. **76**, 1413 (1996); J. Magueijo *et al.*, Phys. Rev. Lett. **76**, 2617 (1996).  
[29] J. C. Magueijo, Phys. Rev. **D46**, 3360 (1992).